Available online at www.sciencedirect.com
SCIENCE DIRECT®
PERGAMON
Solid State Communications 127 (2003) 131–139
solid state communications
www.elsevier.com/locate/ssc

Mn_{12}-acetate: a prototypical single molecule magnet

K.M. Mertes[a], Y. Suzuki[a], M.P. Sarachik[a,*], Y. Myasoedov[b], H. Shtrikman[b], E. Zeldov[b], E.M. Rumberger[c], D.N. Hendrickson[c], G. Christou[d]

[a]*Physics Department, City College of the City University of New York, New York, NY 10031, USA*
[b]*Department of Condensed Matter Physics, The Weizmann Institute of Science, Rehovot 76100, Israel*
[c]*Department of Chemistry and Biochemistry, University of California at San Diego, La Jolla, CA 92093, USA*
[d]*Department of Chemistry, University of Florida, Gainesville, FL 32611, USA*

Received 1 April 2003

Abstract

Single molecule magnets display fascinating quantum mechanical behavior, and may have important technological applications for information storage and quantum computation. A brief review is given of the physical properties of Mn_{12}-acetate, one of the two prototypical molecular nanomagnets that have been most intensively investigated. Descriptions and discussions are given of the Mn_{12} magnetic cluster and the fundamental process of quantum tunneling of a nanoscopic spin magnetization; the distinction between thermally-assisted tunneling and pure quantum tunneling, and a study of the crossover between the two regimes; and a review of earlier investigations that suggest that the tunneling in this system is due to locally varying second-order crystal anisotropy which gives rise to a distribution of tunnel splittings. In the second part of the paper, we report results obtained by a new experimental method that confirm our earlier conclusion that the tunnel splittings in Mn_{12} are distributed rather than single-valued, as had been generally assumed.

PACS: 75.50.Xx; 75.45.tj

Keywords: A. Organic crystals; A. Insulators; D. Tunneling

There has been a great deal of recent interest in nanoscale magnetic phenomena. Remarkable progress has been made in the nanofabrication, control and study of such systems, leading to significant advances in our ability to test fundamental theoretical concepts in quantum mechanics and magnetism. In addition to their intrinsic interest, magnetic phenomena on this scale may have significant technological impact as nanoscale memory elements and as qubits for quantum computation.

A unique and very promising avenue for the study of nanoscale magnetism is provided by molecular nanomagnets, sometimes referred to as single molecule magnets. These organic materials contain a very large (Avogadro's) number of nearly identical magnetic molecules that provide ideal laboratories for the study of nanoscale magnetic phenomena. Although many such molecules have been synthesized in the past few years, much effort has been focused on the study of two particular systems: Mn_{12}-acetate [1], and Fe_8 [2]. The magnetic relaxation in these two systems take place on an intermediate time scale (neither too long nor extremely short) that is amenable to measurement.

Indeed, there have been a number of remarkable findings in Mn_{12} and Fe_8: regular steps in the hysteresis associated with magnetic relaxation via quantum tunneling [3–6], quantum interference effects (Berry's phase) in the magnetic relaxation of Fe_8 [7], quantum avalanches in Mn_{12} [8,9], coherent quantum oscillations of the spin between degenerate ground state minima in Fe_8 [10], and evidence of an abrupt transition between classical over-the-barrier magnetic relaxation and magnetic relaxation by quantum tunneling in Mn_{12} [11–13].

In this paper, we focus our attention on the properties of $([Mn_{12}O_{12}(CH_3COO)_{16}(H_2O)_4]\cdot 2CH_3COOH\cdot 4H_2O)$, referred to as Mn_{12}-acetate. We first present some

* Corresponding author.
E-mail address: sarachik@sci.ccny.cuny.edu (M.P. Sarachik).

0038-1098/03/$ - see front matter © 2003 Elsevier Science Ltd. All rights reserved.
doi:10.1016/S0038-1098(03)00344-2

background and a description of the molecule, and then review some of the interesting physics, including the nature of the crossover between thermally-activated and quantum tunneling, and the symmetry-breaking terms that drive the tunneling in this material. In the second half of the paper, we present a detailed report of data obtained by a new method that yields evidence that the tunnel splittings of the Mn_{12} molecules are distributed rather than single-valued, and we obtain information about the distribution.

First synthesized in 1980, Mn_{12}-acetate received little attention until its magnetic bistability was realized [1]. It contains magnetic clusters composed of twelve Mn ions (see Fig. 1) coupled by superexchange through oxygen bridges to give a sizable $S = 10$ spin magnetic moment that is stable at temperatures of the order of 10 K and below. The identical weakly interacting clusters are regularly arranged on a tetragonal crystal lattice. As shown by the double well potential of Fig. 2(a), strong uniaxial anisotropy of the order of 60 K yields doubly degenerate ground states in zero field and a set of excited levels corresponding to different projections, $m_s = \pm 10, \pm 9, \ldots, 0$, of the total spin along the easy c-axis of the crystal. Below the blocking temperature of 3 K, a series of steps [3–5] are observed in the magnetization M as a function of magnetic field H_z applied along the anisotropy axis, as shown in Fig. 3. These steps occur at roughly equal intervals of magnetic field and are due to enhanced relaxation of the magnetization whenever levels on opposite sides of the anisotropy barrier coincide in energy. As shown in Fig. 3, the curves are different at different temperatures above 0.5 K, indicating that thermal effects play a role, while below 0.5 K the magnetization curves coincide so that essentially all the tunneling proceeds from the ground state of the metastable well. Above 0.5 K, the relaxation proceeds by thermally-assisted quantum tunneling [4,14] of the spin magnetization: the spin is thermally activated to a level above the ground state in the metastable potential well from which it tunnels across the barrier. At the lowest temperatures, tunneling proceeds from the ground state only, requiring no thermal assistance. Fig. 4 shows the steps observed for tunneling from the ground state at low temperature, and the first derivative $\partial M/\partial H$ which displays maxima corresponding to enhanced tunneling at the resonant magnetic fields.

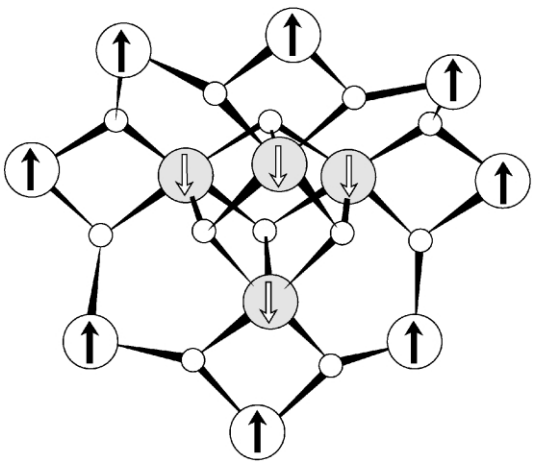

Fig. 1. Schematic diagram of the Mn_{12} molecule. The four inner spin-down Mn^{3+} ions each have spin $S = 3/2$, the eight outer spin-up Mn^{4+} ions each have spin $S = 2$, to give a net spin $S = 10$ for the magnetic cluster.

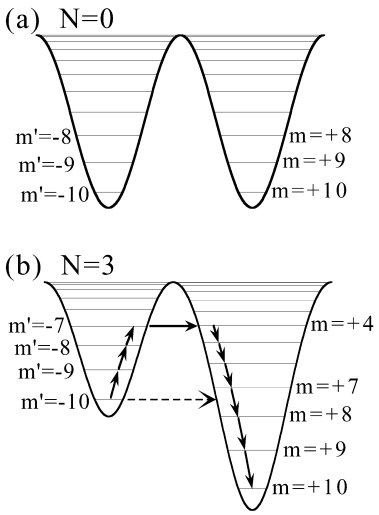

Fig. 2. Schematic diagram of double-well potential: (a) in the absence of an external magnetic field, and (b) in the presence of a magnetic field applied in the direction of the uniaxial c-axis of the Mn_{12} crystal for step $N = 3$. The solid arrows indicate thermally-assisted tunneling and the dotted line denotes tunneling from the ground state of the metastable well. Due to the presence of the small fourth order term, AS_z^4, in the Hamiltonian (see Eq. (1)), different pairs (m', m) of energy levels cross at different magnetic fields. Thus, as indicated in the figure, the pair $(-7,4)$ comes into resonance at a lower magnetic field than the pair $(-10,7)$.

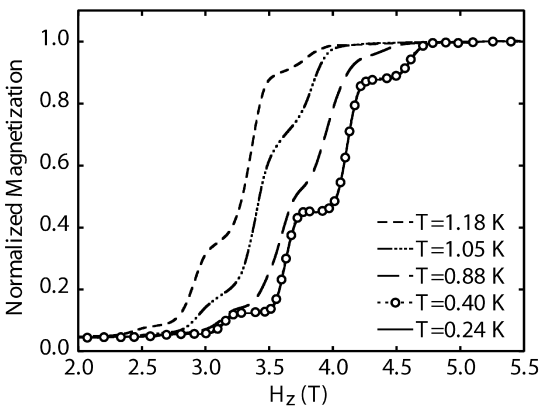

Fig. 3. The magnetization of Mn_{12}-acetate as a function of magnetic field at five different temperatures. The symbols are shown for clarity, and represent a subset of the available data.

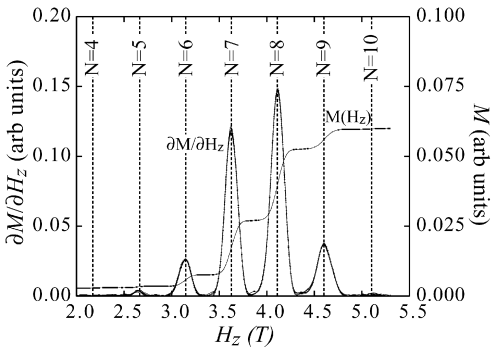

Fig. 4. The magnetization and its first derivative for tunneling from the ground state of the metastable potential well at temperatures below 0.5 K. The maxima correspond to rapid tunneling for different step numbers N where levels coincide on opposite sides of the anisotropy barrier.

The Hamiltonian for Mn_{12}-acetate is given by:

$$\mathscr{H} = -DS_z^2 - AS_z^4 - g_z\mu_B H_z S_z + \mathscr{H}_T, \tag{1}$$

where $\mathscr{H}_T$ contains all symmetry-breaking terms responsible for the tunneling. EPR [15,16] and neutron scattering [17–19] experiments have yielded precise values of the anisotropy $D = 0.548(3)$ K, the fourth-order longitudinal anisotropy $A = 1.173(4) \times 10^{-3}$ K, and an estimate for g_z of 1.94(1). Tunneling occurs from level m' in the metastable well to level m in the stable potential well for magnetic fields:

$$H_z = N\frac{D}{g_z\mu_B}\left[1 + \frac{A}{D}(m^2 + m'^2)\right]. \tag{2}$$

In the absence of the second term in the square brackets, all pairs of levels shown in Fig. 2(b) would cross at the same magnetic field. However, due to the small fourth-order longitudinal term, AS_z^4, each step $N = |m + m'|$ is split into a set of non-simultaneous level crossings at closely spaced magnetic fields, depending on (m, m'), with levels near the top crossing at the smaller magnetic fields. Comparison of the measured magnetic fields with those calculated from Eq. (2) therefore provides an experimental tool that allows identification of the states that are predominantly responsible for the tunneling. One expects most of the tunneling to occur at levels near the top of the potential barrier at higher temperatures, and near the bottom at very low temperatures.

Thermal activation becomes exponentially more difficult as one proceeds up the ladder to higher energy levels; on the other hand, the barrier is lower and more penetrable, so that the tunneling process becomes exponentially easier. Which level (or group of adjacent levels) dominates the tunneling is determined by competition between the two effects. Chudnovsky and Garanin [20–22] proposed that as the temperature is reduced, the levels that dominate the tunneling can shift to lower energies either continuously ('second-order' transition) or abruptly ('first order' transition in the limit $S \to \infty$ and $T \to 0$), depending on the form of the potential.

The crossover with decreasing temperature is shown in Figs. 5 and 6. Fig. 5 shows $\partial M/\partial H_z$ for step $N = 7$ as a function of magnetic field H_z at various different temperatures T; Fig. 6 shows a three-dimensional view as a function of T and magnetic field H_z; here the larger values of $\partial M/\partial H_z$ are denoted by the lighter shading, corresponding to faster magnetic relaxation. Steps $N = 6$, 8, and 9 show similar behavior. There is an abrupt transfer of weight over a narrow range of temperature to a magnetic field that agrees quantitatively with the calculated position for tunneling from $m' = -10$, while tunneling at the field calculated for the $m' = -9$ level appears to be suppressed or entirely absent. Experiment thus indicates that there is indeed an abrupt crossover to tunneling from the lowest state of the metastable well [11–13]. A broad distribution of tunnel splittings, discussed later in this paper, may also contribute to this effect [23].

We now consider what drives the observed tunneling in Mn_{12}-acetate, a long-standing puzzle on which there has been considerable recent progress. In order for tunneling to occur, the Hamiltonian must contain terms that do not commute with S_z. In a perfect crystal, the lowest transverse anisotropy term allowed by the tetragonal symmetry of Mn_{12} is proportional to $(S_+^4 + S_-^4)$. For ground state tunneling, such a term only permits every fourth step. In contrast, all steps are observed with no clear differences in amplitude between them. This suggests that transverse internal magnetic fields, which would allow all steps to occur on an equal footing, provide the dominant symmetry-breaking term that drives the tunneling in Mn_{12}. However, dipolar fields [24–27] and hyperfine interactions [24,28,29] by themselves are too weak to cause the rapid tunneling rates observed.

A recent study [30] of the magnetic relaxation due to ground state tunneling at temperatures below 0.5 K for different sweep rates of a magnetic field applied along the

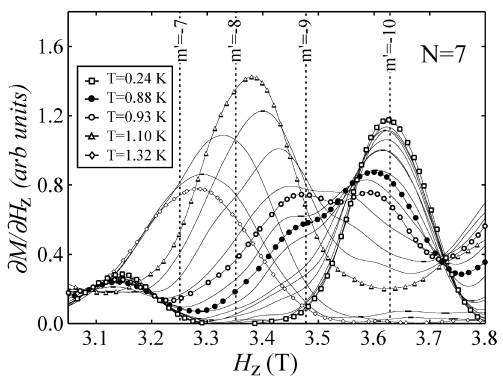

Fig. 5. $\partial M/\partial H_z$ for step $N = |m' + m| = 7$ as a function of magnetic field H_z at various different temperatures T. The vertical lines denote crossings of different pairs of levels (m', m). The symbols are shown for clarity, and represent a subset of the available data.

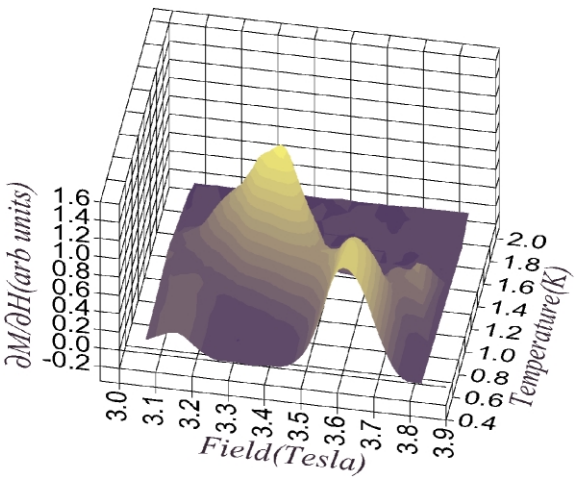

Fig. 6. Three-dimensional plot of $\partial M/\partial H_z$ for step $N = |m' + m| = 7$ as a function of magnetic field H_z and temperature T.

longitudinal (easy) axis has yielded evidence for a broad distribution of tunneling splittings. Typical data are shown in Fig. 7. An approximate collapse of the data onto a single curve, shown in Fig. 8, is obtained for a scaling form proposed by Garanin and Chudnovsky [31,32] for tunneling due to broadly distributed second-order transverse anisotropy that varies locally throughout the Mn_{12} crystal. We attribute the small departures from perfect scaling to the admixture of tunneling due to other symmetry-breaking terms, such as transverse internal magnetic fields and fourth

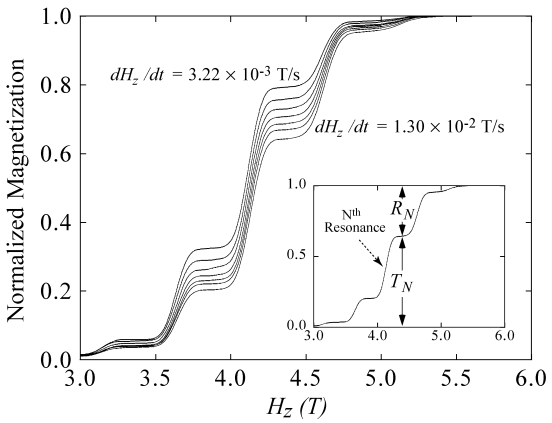

Fig. 7. Normalized magnetization curves at 0.24 K for sweep rates ranging from 1.30×10^{-2} T/s to 3.22×10^{-3} T/s in roughly equal intervals. For a broad distribution of tunnel splittings, the normalized magnetization at a plateau, labeled T_N in the inset, represents the cumulative fraction of molecules that have tunneled (relaxed) after an energy level in the metastable well has come into resonance with an energy level in the stable well; $R_N = 1 - T_N$ is the fraction of molecules that remain in the metastable well after the Nth level crossing.

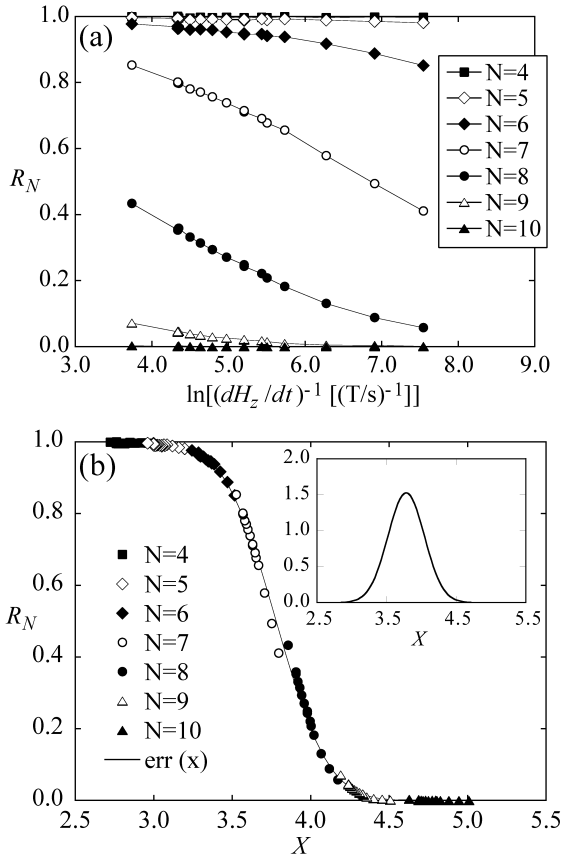

Fig. 8. Part(a) shows the fraction of remaining molecules, R_N, determined as indicated in the inset of Fig. 7, plotted for each resonance N versus the natural logarithm of the inverse sweep rate for various sweep rates ranging from 0.53 to 23.7 mT/s. Part (b) shows that R_N scales onto one curve when plotted as a function of the scaling parameter, X, shown in Ref. [30] to be independent of N for tunneling driven by second-order crystal anisotropy, $X = -\ln(|E|/2D)$. The solid continuous curve is a best fit to the data using the error function. The inset illustrates the log-Gaussian distribution of transverse anisotropies determined by taking the derivative of the scaled curve.

order crystalline anisotropy. Thus,

$$\mathscr{H} = \cdots + E(S_x^2 - S_y^2) - g_x \mu_B H_x S_x, \tag{3}$$

with $E = E(x, y, z)$ and $H_x = H_x(x, y, z)$ varying from point to point in the Mn_{12} crystal. These results imply that the dominant term responsible for tunneling is second-order anisotropy which, although prohibited in a perfect crystal, is present and significant in real crystals of Mn_{12}. Evidence has been provided by recent ESR [33] and terahertz experiments [34] that the longitudinal parameters D, A and g_z (see Eq. (1)) are also distributed.

In the remainder of this paper, we present some recent results that provide additional strong evidence that the tunnel splittings are distributed. These results are obtained using a new experimental protocol where the magnetic

relaxation of Mn_{12}-acetate is investigated in a longitudinal field that is swept back and forth across each resonant step. This new method yields experimental verification that the tunnel splittings are distributed, and provides a tool for determining the form of the distribution.

The magnetization of small single crystals of Mn_{12}-acetate was determined from measurements of the local magnetic induction at the sample surface using $10 \times 10\ \mu m^2$ Hall sensors composed of a two-dimensional electron gas (2DEG) in a GaAs/AlGaAs heterostructure. The 2DEG was aligned parallel to the external magnetic field, and the Hall sensor was used to detect the perpendicular component (only) of the magnetic field arising from the sample magnetization [35].

The relaxation of the magnetization was studied for each observable ground state resonance: starting from zero magnetization, the external field was swept from zero up to and beyond a given resonance N. When the field reached the middle of the plateau just above step N, it was reversed and swept back across this resonance. When the field reached the middle of the previous plateau, the field was swept back up, and the process was repeated many times [36]. The same procedure was repeated for all observed resonances, $N = 4, 5, \ldots, 9$, as shown in the normalized magnetization curves of Fig. 9 [37]. The turning points were chosen so that the amplitude of the field oscillations were the same for each N and the turning points of the field occurred near the center of a plateau. The field was swept at a rate $|dH_z/dt| = 7.15$ mT/s. Note that full magnetization was not reached for the lower-numbered steps due to the finite (8 h) holding time of the ^{3}He refrigerator.

As the field is swept back and forth across the resonance, the magnetization relaxes in steps. The manner in which it relaxes is expected to be different for a set of identical molecules than for the case of a distribution of tunnel splittings. We show below that an ensemble of identical molecules cannot describe the data. A method of fitting different distributions to the magnetization data is developed, and an excellent fit is obtained for a distribution that varies from log-normal Gaussian to Gaussian. We also argue that dipolar shuffling [38] would produce an asymmetry in the steps which is not observed.

The fraction of molecules remaining after each step can be determined from the magnetization curves. At the turning points labeled by $f_0, f_1, f_2, \ldots$, for $N = 7$, shown in the inset to Fig. 9, the fraction of molecules remaining in the metastable well is related to the normalized magnetization by

$$f_j = (1 - M_j)/2, \tag{4}$$

where M_j is the normalized magnetization at the turning points of the field. For each N, Fig. 10 shows the fraction of molecules remaining in the metastable well after each field pass plotted as a function of how many times, j, the field was swept past the resonance. The issue is whether or not the fraction remaining after each field sweep is consistent with the behavior expected for a sample comprised of an ensemble of identical molecules.

For a set of identical molecules, the probability, P_N, of remaining in the metastable well for resonance, N, is the same for each molecule. If the fraction of molecules in the metastable well before sweeping past the Nth resonance is $f_{N,0}$, then the fraction of molecules remaining in the metastable well after sweeping the field through a resonance will be $f_{N,1} = f_{N,0}P_N$. When the field is swept downward across the resonance a second time, another set of molecules will tunnel. The fraction remaining after the second pass can be determined from the fraction remaining after the first pass, $f_{N,2} = f_{N,1}P_N = f_{N,0}(P_N)^2$. In general, the fraction of molecules remaining in the metastable well after j passes of

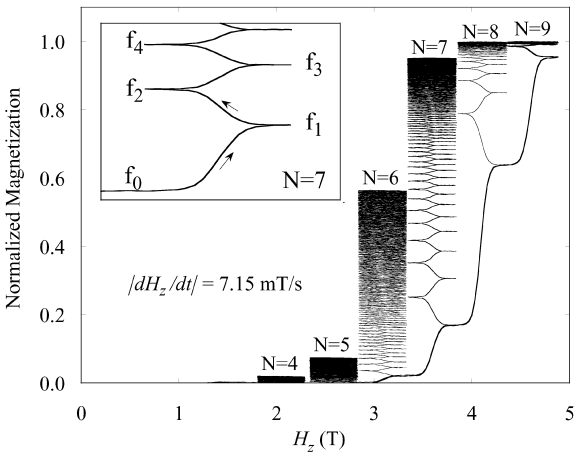

Fig. 9. Normalized magnetization versus magnetic field for a field that is swept back and forth across each resonance. The field was swept at a rate of $|dH_z/dt| = 7.15$ mT/s. The inset shows the labeling described in the text for the first few oscillations for step $N = 7$. Data were taken at 0.24 K.

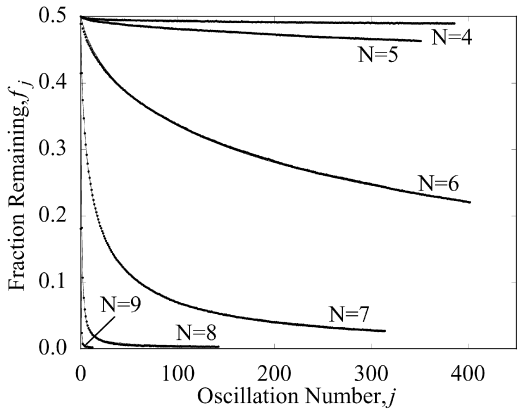

Fig. 10. The fraction of molecules remaining in the metastable well as a function of the oscillation number, j. The distributions of tunnel splittings specified in the text provide fits to Eq. (6) for each N shown by the solid lines that are nearly indistinguishable from the measured data.

the field is:

$$f_{N,j} = f_{N,0}(P_N)^j. \quad (5)$$

This form implies that for a set of identical molecules, $f_{N,j}$ would depend exponentially on j, and a semi-logarithmic plot of the remaining fraction, $f_{N,j}$, versus the number of oscillations, j, should yield straight lines for each N. As can be seen in Fig. 11, which shows the data of Fig. 10 on a semi-logarithmic scale, this is not the case. The simple assumption that all the molecules are identical is clearly inconsistent with the data.

We now consider the case of a distribution of tunnel splittings. A possible source of such a distribution is a locally varying, broadly distributed transverse second-order anisotropy which is forbidden by the tetragonal symmetry of the Mn_{12}-acetate crystal, but which is present in real crystals. Chudnovsky and Garanin [31,32] have proposed that long-range crystal dislocations produce deformations that require inclusion of a magnetoelastic term in the Hamiltonian, giving rise to a transverse anisotropy, $E(S_x^2 - S_y^2)$ that varies with the distance from the dislocation. Alternatively, Cornia et al. [39] have pointed out that there are six different isomers of Mn_{12}-acetate, four of which are only two-fold symmetric. This lowers the symmetry group for the Hamiltonian and also permits inclusion of locally varying second-order transverse anisotropy terms. Another possible source is a distribution due to transverse fields, $H_\perp$, of either dipolar or hyperfine origin. Recent experiments have shown that the chemical isomers are at least partly responsible for the observations [40,41]. The analysis below is valid regardless of the origin of the distribution of tunnel splittings.

The probability of remaining in the metastable well is given [21,42] by the formula $P_N(\Delta) = \exp(-\pi\Delta^2/2\hbar|v_N|)$,

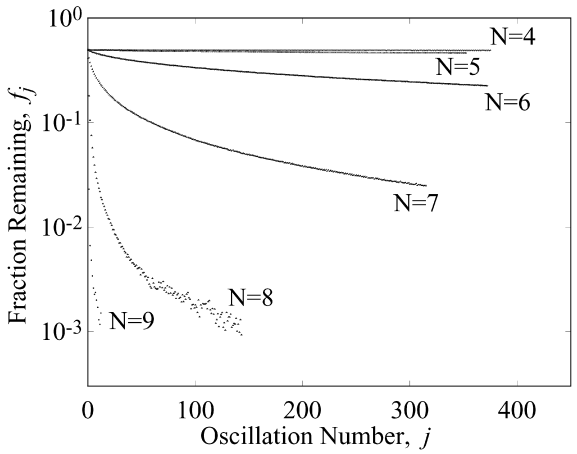

Fig. 11. The fraction of molecules remaining in the metastable well as a function of the oscillation number, j, plotted on a semi-logarithmic scale. The data are inconsistent with an ensemble of identical molecules (see text), for which the fraction f_j is expected to vary exponentially with j and yield a straight line on this plot.

where Δ is the tunnel splitting and $v_N = (2S - N)g_z\mu_B dH_z/dt$ is the energy sweep rate. For an arbitrary initial distribution of tunnel splittings for the Nth resonance, $\tilde{f}_{N,0}(\Delta)$, the fraction of molecules remaining in the metastable well with a tunnel splitting between Δ and $\Delta + d\Delta$ is $\tilde{f}_{N,1}(\Delta)d\Delta = P_N(\Delta)\tilde{f}_{N,0}(\Delta)d\Delta$. Integrating over all possible tunnel splittings, one obtains the fraction of molecules remaining in the metastable well after having swept the field entirely through the resonance, $f_{N,1} = \int_0^\infty \times P_N(\Delta)\tilde{f}_{N,0}(\Delta)d\Delta$. In general, the total fraction of molecules remaining in the metastable well after sweeping the field back and forth across the Nth resonance j times is

$$f_{N,j} = \int_0^{+\infty} (P_N(\Delta))^j \tilde{f}_{N,0}(\Delta)d\Delta. \quad (6)$$

Note that to reach the Nth resonance starting from zero, the field is swept once through each of the lower resonances. Therefore, the initial distribution, $\tilde{f}_{N,0}$, is normalized to the fraction of molecules remaining in the metastable well just before reaching the Nth resonance.

Eq. (6) can be used to model the data shown in Fig. 10. Different initial distributions, $\tilde{f}_{N,0}(\Delta)$, can be chosen and each curve in Fig. 10 should be fit by adjusting the parameters defining the shape of $\tilde{f}_{N,0}(\Delta)$. An excellent fit to the data is obtained for a log-Gaussian distribution of the form [30] $\tilde{f}_{N,0}(\Delta) \propto (1/\Delta)e^{-\ln^2(\Delta/\Delta_0)/4\sigma^2}$. This form captures the behavior remarkably well for resonances, $N = 4$, 5, × 6 and 7 and is indistinguishable from the data shown in Figs. 10 and 11. However, a better fit was obtained for $N = 8$ and 9 by using the Gaussian distribution, $\tilde{f}_{N,0}(\Delta) \propto e^{-(\Delta-\Delta_0)^2/4\sigma^2}$. The evolution from log-Gaussian to Gaussian is due to the fact that for higher numbered steps, a significant portion of the distribution of molecules has already tunneled when the field is swept through the lower resonances. In other words, for large N the portion of the distribution belonging to large Δ is missing since these molecules already tunneled during the lower $N - 1$ resonances. Thus the distribution is no longer symmetric (on a logarithmic scale) and becomes more Gaussian-like.

The distribution for each N shown in Fig. 12 has been normalized to the fraction of molecules remaining in the metastable well just before reaching the Nth resonance; this gives the history-dependent distribution of tunnel splittings for the particular sweep rate used. The inset shows the full width at half maximum (FWHM) for each N plotted on a logarithmic scale.

'Dipolar shuffling' has been recently proposed as an explanation for an unexpected dependence of tunnel splittings on sweep rate [38]. This effect refers to the fact that when a molecule tunnels, the internal dipole fields are locally altered so that some molecules that were previously below are now above the resonance field and vice-versa. The average number of molecules that move above the resonance field compared with the average number of molecules that move below the resonance field depends upon the geometry of the sample. For the long thin sample

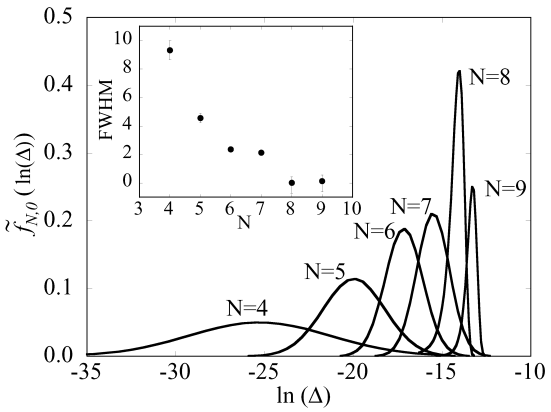

Fig. 12. The distribution of tunnel splittings determined by fitting Eq. (6) to the data depicted in Fig. 10 plotted as a function of ln(Δ). The inset shows FWHM (full width at half maximum) of each distribution.

studied here ($a \approx 40$ μm, $b \approx 40$ μm, $c \approx 150$ μm), this is expected to introduce an asymmetry between up- and down-sweeps: during an up-sweep many of the dipole-shuffled molecules will skip the resonant field resulting in a lower tunneling rate while during a down-sweep molecules will have additional opportunities to tunnel giving an enhanced tunneling rate. This would yield a tilted staircase behavior in the fraction of molecules with successive values of j. Fig. 13 shows that the fraction remaining varies smoothly with oscillation number and does not exhibit a tilted staircase behavior. In addition, according to Liu et al. [38], dipolar shuffling will only occur when the field is swept slowly enough. In particular, the energy sweep rate, $v_N = g_z\mu_B(2S-N)\mathrm{d}H_z/\mathrm{d}t$ must be smaller than the characteristic energy rate, $\pi\Delta_N^2/\hbar$.

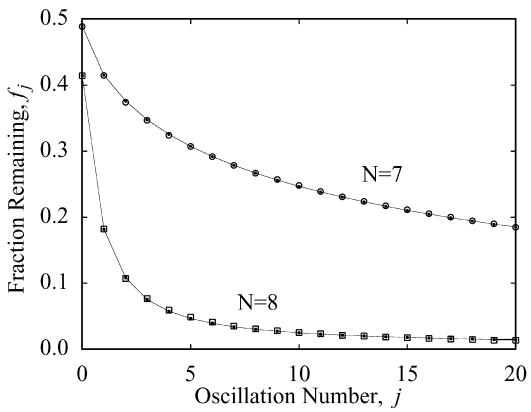

Fig. 13. The fraction of molecules remaining in the metastable well as a function of the oscillation number, j, for $N = 7$ and $N = 8$ plotted on an expanded scale. The larger hollow symbols are the measured values and the smaller solid symbols are theoretical values. The solid line connects successive theoretical values. The fact that the data vary smoothly with oscillation number, j, indicates that dipolar shuffling has a minimal effect on the data.

Table 1
Comparison of the energy rate, $\pi\Delta_N^2/\hbar$ with the energy sweep rate, $v_N = g_z\mu_B(2S-N)\mathrm{d}H_z/\mathrm{d}t$. Dipolar shuffling should occur when $v_N < \pi\Delta_N^2/\hbar$

N	$\pi\Delta_N^2/\hbar$ (K/s)	v_N (K/s)
4	2.86×10^{-11}	1.22×10^{-1}
5	7.11×10^{-7}	1.14×10^{-1}
6	5.77×10^{-4}	1.06×10^{-1}
7	1.39×10^{-2}	9.88×10^{-2}
8	1.91×10^{-1}	9.12×10^{-2}
9	6.59×10^{-1}	8.36×10^{-2}

Table 1 lists the energy rate and energy sweep rate defined above for steps $N = 4, \ldots, 9$. These numbers indicate that if dipolar shuffling were the chief source of the non-exponential decay, then the fraction of molecules remaining should relax exponentially for $N < 8$ and relax non-exponentially for $N \geq 8$. Since the fraction remaining relaxes non-exponentially for all N and does not exhibit the expected staircase behavior, we conclude that for the samples studied here, there was no observable effect associated with dipolar shuffling. Thus, dipolar shuffling is not responsible for the non-exponential behavior shown in Fig. 11.

Fig. 13 shows the quality of the fit of Eq. (6) (i.e. under the assumption of a distribution of tunnel splittings). The larger hollow symbols are the measured fraction of molecules remaining for steps $N = 7$ and $N = 8$. The smaller solid symbols are the fraction remaining determined from Eq. (6). The theoretical fit is nearly indistinguishable from the measured data. The solid lines connecting successive theoretical fits are drawn as an aide to illustrate the non-exponential behavior as well as to show that dipolar shuffling is a small effect.

To recap the last portion of this paper, the dependence of the measured tunneling probability on the amount of magnetization remaining in the metastable potential well was studied by sweeping the field back and forth across each field resonance N. The fraction of molecules remaining in the metastable well after each sweep through the resonance was shown to be consistent with a distribution of tunnel splittings. This new experimental protocol provides a method for determining the form of the distribution. Similar experiments in Mn_{12}-acetate using magnetic field that is repeatedly swept back and forth across a single resonance have recently been reported by del Barco et al. [43].

We have briefly reviewed the structure and some of the interesting physical properties of Mn_{12}-acetate, one of the two prototypical molecular nanomagnets that have been most intensively investigated. The fundamental process of quantum tunneling of a nanoscopic spin magnetization was described. We discussed thermally-assisted tunneling, pure quantum tunneling from the ground state, and the crossover between them. Data obtained by two different experimental methods provide strong evidence that the tunnel splittings,

which had heretofore been assumed to be identical for all magnetic molecules in the crystal, are instead broadly distributed due to locally varying second-order crystal anisotropy.

In contrast with Mn_{12}, which is uniaxial on a long length scale, the tunneling in Fe_8 is associated with long range second-order crystal anisotropy which provides inequivalent tunneling paths over the barrier in the hard plane. This feature was exploited in a beautiful experiment by Wernsdorfer and Sessoli [7] to demonstrate interference effects associated with Berry's phase.

Much effort is currently being devoted to synthesize new and different molecular magnets with different properties, larger spin and larger barriers. These materials are of great interest for physical properties that are borderline between classical and quantum mechanical behavior, and because they may have important technological applications for high density storage of information and, perhaps, for quantum computation.

Acknowledgements

We thank Nurit Avraham for many insightful comments, and for help in preparing the manuscript. Work at City College was supported by NSF grant DMR-0116808 and at the University of California, San Diego by NSF grants CHE-0095031 and DMR-0103290. Support for G. C. was provided by NSF grants DMR-0103290 and CHE-0123603. E. Z. and H. S. acknowledge the support of the Israel Science Foundation Center of Excellence grant 8003/02.

References

[1] R. Sessoli, D. Gatteschi, A. Caneschi, M.A. Novak, Nature 365 (1993) 141–143.
[2] A.L. Barra, P. Debrunner, D. Gatteschi, C.E. Schulz, R. Sessoli, Europhys. Lett. 35 (1996) 133.
[3] J.R. Friedman, M.P. Sarachik, J. Tejada, R. Ziolo, Phys. Rev. Lett. 76 (1996) 3830. J.M. Hernandez, X.X. Zhang, F. Luis, J. Bartolome, J. Tejada, R. Ziolo, Europhys. Lett. 35 (1996) 301.
[4] J.R. Friedman, PhD Thesis. The City University of New York, 1996.
[5] L. Thomas, F. Lionti, R. Ballou, D. Gatteschi, R. Sessoli, B. Barbara, Nature (London) 383 (1996) 145.
[6] C. Sangregorio, T. Ohm, C. Paulsen, R. Sessoli, D. Gatteschi, Phys. Rev. Lett. 78 (1997) 4645.
[7] W. Wernsdorfer, R. Sessoli, Science 284 (1999) 133.
[8] C. Paulsen, J.-G. Park, in: L. Gunther, B. Barbara (Eds.), Quantum Tunneling of Magnetization, Kluwer, Dordrecht, 1995.
[9] E. del Barco, J.M. Hernandez, M. Sales, J. Tejada, H. Rakoto, J.M. Broto, E.M. Chudnovsky, Phys. Rev. B 60 (1999) 11898.
[10] E. del Barco, N. Vernier, J.M. Hernandez, J. Tejada, E.M. Chudnovsky, E. Molins, G. Bellessa, Europhys. Lett. 47 (1999) 722.
[11] A.D. Kent, Y. Zhong, L. Bokacheva, D. Ruiz, D.N. Hendrickson, M.P. Sarachik, Europhys. Lett. 49 (2000) 521.
[12] L. Bokacheva, A.D. Kent, M.A. Walters, Phys. Rev. Lett. 85 (2000) 4803.
[13] K.M. Mertes, Y. Zhong, M.P. Sarachik, Y. Paltiel, H. Shtrikman, E. Zeldov, E. Rumberger, D.N. Hendrickson, G. Christou, Europhys. Lett. 55 (2001) 874.
[14] M.A. Novak, R. Sessoli, in: L. Gunther, B. Barbara (Eds.), Quantum Tunneling of Magnetization, Kluwer, Dordrecht, 1995.
[15] A.L. Barra, D. Gatteschi, R. Sessoli, Phys. Rev. B 56 (1997) 8192.
[16] S. Hill, J.A.A.J. Perenboom, N.S. Dalal, T. Hathaway, T. Stalcup, J.S. Brooks, Phys. Rev. Lett. 80 (1998) 2453.
[17] Y. Zhong, M.P. Sarachik, J.R. Friedman, R. A. Robinson, T.M. Kelley, H. Nakotte, A.C. Christianson, F. Trouw, S.M.J. Aubin, D.N. Hendrickson, J. Appl. Phys. 85 (1999) 5636.
[18] M. Hennion, L. Pardi, I. Mirebeau, E. Suard, R. Sessoli, A. Caneschi, Phys. Rev. B 56 (1997) 8819.
[19] I. Mirebeau, M. Hennion, H. Casalta, H. Andres, H.U. Güdel, A.V. Irodova, A. Caneschi, Phys. Rev. Lett. 83 (1999) 628.
[20] E.M. Chudnovsky, D.A. Garanin, Phys. Rev. Lett. 79 (1997) 4469.
[21] D.A. Garanin, E.M. Chudnovsky, Phys. Rev. B 56 (1997) 11102.
[22] D.A. Garanin, X. Martinez-Hidalgo, E.M. Chudnovsky, Phys. Rev. B 57 (1998) 13 639.
[23] K.M. Mertes, Y. Suzuki, M.P. Sarachik, Y. Paltiel, H. Shtrikman, E. Zeldov, E.M. Rumberger, D.N. Hendrickson, G. Christou, Phys. Rev. B 65 (2002) 212401.
[24] N.V. Prokof'ev, P.C.E. Stamp, Phys. Rev. Lett. 80 (1998) 5794.
[25] E.M. Chudnovsky, Phys. Rev. Lett. 84 (2000) 5676.
[26] N.V. Prokof'ev, P.C.E. Stamp, Phys. Rev. Lett. 84 (2000) 5677.
[27] W. Wernsdorfer, C. Paulsen, R. Sessoli, Phys. Rev. Lett. 84 (2000) 5678.
[28] F. Hartmann-Boutron, P. Politi, J. Villain, Int. J. Mod. Phys. B 10 (1996) 2577.
[29] D.A. Garanin, E.M. Chudnovsky, R. Schilling, Phys. Rev. B 61 (2000) 12204.
[30] K.M. Mertes, Y. Suzuki, M.P. Sarachik, Y. Paltiel, H. Shtrikman, E. Zeldov, E.M. Rumberger, D.N. Hendrickson, G. Christou, Phys. Rev. Lett. 87 (2001) 227205.
[31] E.M. Chudnovsky, D.A. Garanin, Phys. Rev. Lett. 87 (2001) 187203.
[32] D.A. Garanin, E.M. Chudnovsky, Phys. Rev. B 65 (2002) 94423.
[33] K. Park, M.A. Novotny, N.S. Dalal, S. Hill, P.A. Rikvold, Phys. Rev. B 65 (2002) 14426.
[34] B. Parks, J. Loomis, E. Rumberger, D.N. Hendrickson, G. Christou, Phys. Rev. B 64 (2001) 184426.
[35] E. Zeldov, D. Majer, M. Konczykowski, V.B. Geshkenbein, V.M. Vinokur, H. Shtrikman, Nature 375 (1995) 373.
[36] W. Wernsdorfer, R. Sessoli, A. Caneschi, D. Gatteschi, A. Cornia, D. Mailly, A magnetic field was swept back and forth across the $N = 0$ resonance in Fe_8, J. Appl. Phys. 87 (2000) 5481.
[37] The total saturation magnetization was measured after each oscillation series associated with a given step. The saturation magnetization associated with a second species, which

saturates below 1.5 T, was subtracted and the data were normalized by the saturation magnetization of the remainder associated with the main species of Mn_{12}-acetate.

[38] J. Liu, B. Wu, L. Fu, R.B. Diener, Q. Niu, Phys. Rev. B 65 (2002) 224401.

[39] A. Cornia, R. Sessoli, L. Sorace, D. Gatteschi, A.L. Barra, C. Daiguebonne, Phys. Rev. Lett. 89 (2002) 257201.

[40] S. Hill, R.S. Edwards, S.I. Jones, N.S. Dalal, J.M. North, Preprint Cond-Mat/0301599, 2003.

[41] E. del Barco, A.D. Kent, Bull. Am. Phys. Soc. 48 (2003) 1018.

[42] M.N. Leuenberger, D. Loss, Phys. Rev. B 61 (2000) 12200.

[43] E. del Barco, A.D. Kent, E.M. Rumberger, D.N. Hendrickson, G. Christou, Europhys. Lett. 60 (2002) 768.